Molecular Biology of the Cell
Vol. 11, 1687–1696, May 2000

Truncation Mutants of the Tight Junction Protein ZO-1 Disrupt Corneal Epithelial Cell Morphology

Sandra W. Ryeom,* David Paul,† and Daniel A. Goodenough*‡

Departments of *Cell Biology and †Neurobiology, Harvard Medical School, Boston, Massachusetts 02115

Submitted August 17, 1999; Revised February 15, 2000; Accepted March 3, 2000
Monitoring Editor: Martin Schwartz

The tight junction is the most apical intercellular junction of epithelial cells and regulates transepithelial permeability through the paracellular pathway. To examine possible functions for the tight junction-associated protein ZO-1, C-terminally truncated mutants and a deletion mutant of ZO-1 were epitope tagged and stably expressed in corneal epithelial cell lines. Only full-length ZO-1 and one N-terminal truncation mutant targeted to cell borders; other mutants showed variable cytoplasmic distributions. None of the mutants initially disrupted the localization of endogenous ZO-1. However, long-term stable expression of two of the N-terminal mutants resulted in a dramatic change in cell shape and patterns of gene expression. An elongated fibroblast-like shape replaced characteristic epithelial cobblestone morphology. In addition, vimentin and smooth muscle actin expression were up-regulated, although variable cytokeratin expression remained, suggesting a partial transformation to a mesenchymal cell type. Concomitant with the morphological change, the expression of the integral membrane tight junction protein occludin was significantly down-regulated. The localizations of endogenous ZO-1 and another family member, ZO-2, were disrupted. These findings suggest that ZO-1 may participate in regulation of cellular differentiation.

INTRODUCTION

Epithelial cells create selective permeability barriers between different physiological compartments. Selective permeability is the result of regulated transport of molecules through the cytoplasm (the transcellular pathway) and the regulated permeability of the spaces between the cells (the paracellular pathway) (Goodenough, 1999). Intercellular junctions are known to be involved in both the maintenance and regulation of the barrier function and cell–cell adhesion (Anderson and Van Itallie, 1995; Denker and Nigam, 1998). The tight junction (TJ) is the cell–cell junction that regulates the permeability of the paracellular pathway and also divides the cell surface into apical and basolateral compartments (Anderson *et al.*, 1993; Citi, 1993; Denker and Nigam, 1998). Both integral and peripheral plasma membrane proteins are associated with the TJ (Fujimoto, 1995; Furuse *et al.*, 1998a). The integral membrane proteins occludin (Furuse *et al.*, 1993, 1996) and the claudins (Morita *et al.*, 1999) restrict the intercellular space and presumably also generate regulated "channels" for the paracellular passage of ions and small molecules. Both occludin (Balda *et al.*, 1996; McCarthy *et al.*, 1996; Chen *et al.*, 1997; Wong and Gumbiner, 1997) and claudin family members (Furuse *et al.*, 1998b) have been directly demonstrated to be involved in the barrier function of TJs. One member of the claudin family, paracellin-1, has been implicated in the formation of selective Mg^{2+} channels in kidney distal tubules (Simon *et al.*, 1999).

Although many nonintegral membrane proteins have been localized to the TJ by electron microscopy or immunofluorescence (Stevenson and Keon, 1998), their contributions to the structure and function of TJs are unknown. ZO-1 is the first such protein to be identified (Stevenson *et al.*, 1986). In addition to its localization at the TJ, ZO-1 is also found at adherens junctions in cells lacking TJs (Itoh *et al.*, 1991; Howarth *et al.*, 1992). ZO-1 is the defining member of a family of ZO proteins that includes ZO-2 (Beatch *et al.*, 1996) and ZO-3 (Haskins *et al.*, 1998). All of the ZO proteins belong to a larger superfamily of proteins known as the membrane-associated guanylate kinase (MAGuK) family (Anderson and Van Itallie, 1995; Kim, 1995; Anderson, 1996). MAGuK proteins are composed of domains that include: 1) three PDZ domains, which are 90-amino-acid protein–protein binding domains with a repeating GLGF sequence (Cho *et al.*, 1992); 2) an Src homology 3 domain shown in other proteins to bind proline-rich regions (Ren *et al.*, 1993); and 2) a guanylate kinase (GuK) domain that may be enzymatically inactive (Willott *et al.*, 1993). The ZO proteins also contain proline-rich C termini varying in length from 145 to 954 amino acids.

‡ Corresponding author. E-mail address: daniel_goodenough@hms.harvard.edu.

The function of ZO-1 is unknown. Other MAGuK family members have been shown to play roles in clustering receptors or channels in the plasma membrane (Kim *et al.*, 1995), and some PDZ domains have been shown to bind to consensus motifs at the absolute C termini of polypeptides (Songyang *et al.*, 1997). In vitro studies have suggested functions for various domains of ZO-1. For example, the N terminus containing the PDZ and GuK domains targets to cell borders when exogenously expressed in both epithelial and nonepithelial cells, whereas the proline-rich C terminus associates with actin filaments and actin-rich structures (Itoh *et al.*, 1997; Fanning *et al.*, 1998). In addition, these studies revealed domains of ZO-1 that are involved in interactions with ZO-2 and ZO-3 and that the GuK domain interacts with occludin (Itoh *et al.*, 1997; Fanning *et al.*, 1998). It remains unclear whether these interactions are necessary for TJ assembly or function.

Because ZO-1 contains multiple domains believed to be involved in protein–protein interactions, a reasonable approach to disrupting ZO-1 activity is exogenous expression of subsets of these domains. Therefore, we stably expressed epitope-tagged deletion mutants of ZO-1 in corneal epithelial cells. These stable cell lines were then assayed for changes in TJ sealing properties and for cellular localization of both mutants and endogenous ZO-1. After stable expression for >1 mo, two of these mutants induced a morphological change reminiscent of an epithelium-to-mesenchyme transition. These results suggest that N-terminal regions of ZO-1 are able to activate signaling pathways involved in cellular differentiation.

MATERIALS AND METHODS

Cell Culture

SV40 immortalized rabbit and human corneal epithelial (CE) cell lines were generously provided by Dr. K. Araki-Sasaki (Ehime University School of Medicine, Osaka, Japan) and were maintained as previously described (Araki *et al.*, 1993; Araki-Sasaki *et al.*, 1995). Cells were grown in growth medium (Ham's F-12/Dulbecco's modified Eagle's medium, 10% heat-inactivated fetal bovine serum [Hyclone Laboratories, Logan, UT], 5 μg/ml insulin, 0.1 μg/ml cholera toxin, 10 ng/ml epidermal growth factor, 0.5% dimethylsulfoxide, and 40 μg/ml gentamicin) and maintained in a humidified chamber with 5% CO_2 at 37°C.

Mutants

To express mutants containing multiple c-*myc* epitope tags, each mutant was first subcloned into the pCS2+myc vector (generously provided by Dr. M. Klymkowsky, University of Colorado, Boulder, CO) and then subcloned into the expression vector pCDNA 3+ (Invitrogen, Carlsbad, CA). The cDNA containing the entire open reading frame of mouse ZO-1 was kindly provided by Dr. S. Tsukita (Kyoto University, Kyoto, Japan). Full-length ZO-1^{1-1745}, was ligated into the *Cla*I site of pCS2+myc. All other mutants were generated by PCR using mouse ZO-1 cDNA as a template. For ZO-1^{1-263} the sense primer (5′AGC***GGATCC***ATGTCCGCCAGGGCCGCGGCCGCTAAGAGCACAGCAATGGAGGAAACAGCTATATGGGAAC-3′) introduced a *Bam*HI site (bold italics), and an antisense primer (5′-AGCCC***ATCGAT***TCTCATCTCTTTGCACTACCAT-3′) introduced a *Cla*I site (bold italics) at the end of the ZO-1 open reading frame. All of the mutants used the same sense primer with different antisense primers introducing *Cla*I sites (bold italics) downstream of the ZO-1 open reading frame. The antisense primer for ZO-1^{1-422} was 5′-AGC***ATCGAT***CCATGCTGGGCCTAAGTATCC-3′ and for ZO-1^{1-794} was 5′-GATT***ATCGAT***CCTGTTGCTGCTGAATCGCTTCTTT-3′. Each amplified fragment was ligated into the *Bam*HI and *Cla*I sites of pCS2+myc, released with multiple myc epitopes at their C terminus by digestion with *Bam*HI and *Eco*RI, and ligated into the same sites of pCDNA 3+. ZO-$1^{\Delta 615-812}$, with a missing GuK domain, was constructed by PCR amplification of two halves of ZO-1 using the same sense primer as above for the N-terminal half and an antisense primer (5′-AGC***GTCGAC***GGAGCTGCGAAGACCTCGAAA-3′), which puts a *Sal*I site (bold italics) on the 3′ end. The C-terminal half of this mutant was constructed using the sense primer (5′-AGC***GTCGAC***ATGGTGCTACAAGTGATGACC-3′) with a *Sal*I site and an antisense primer (5′-AGC***GAATTC***TTACTTGTCATCGTCGTCCTTGTAGTCAAAGTGGTCAATCAGGACAGA-3′) with an *Eco*RI site (bold italics) and a FLAG epitope (underline) at the end of the open reading frame. The two halves of ZO-$1^{\Delta 615-812}$ were ligated together at their *Sal*I sites and into the *Bam*HI–*Eco*RI site of pCDNA 3+.

Transfection and Generation of Stable Lines

Corneal epithelial cells were transfected with 1 μg of each mutant using LipofectAMINE Plus reagent (Life Technologies, Rockville, MD) for 12 h in F-12/Dulbecco's modified Eagle's medium. After this incubation, the transfection medium was changed to growth medium (see above) and allowed to grow for 48 h. Cells were split into 60-mm dishes in the presence of 800 μg/ml geneticin (Life Technologies) to select stable transfectants. After three independent transfection experiments of the various truncation mutants into corneal epithelial cells, single cells were isolated by limiting dilution into 96-well plates. Clones were expanded and screened by immunofluorescence with either a c-*myc* mouse monoclonal antibody (Calbiochem, La Jolla, CA) or a mouse monoclonal FLAG antibody (Eastman Kodak, Rochester, NY). Six to 24 independent clones for each mutant were isolated and examined with similar results. Transfected cells were retrieved from frozen stocks on three separate occasions, recloned, and followed for 4–6 wk to ensure the reproducibility of the phenotypic change. Although both rabbit and human corneal epithelial cells were used for all experiments, the data shown are from rabbit epithelial cells.

Immunofluorescence

Cells plated on Nunc Lab Tek glass chamber slides (VWR, Boston, MA) were washed with PBS two times and fixed with 1% formaldehyde in PBS for 20 min. The fixed cells were blocked and permeabilized with 0.2% Triton-X 100 in 5% normal goat serum for 45 min. The samples were then treated with primary antibodies including ZO-1, ZO-2, and occludin rabbit polyclonal antibodies and vimentin, cytokeratin, and smooth muscle actin monoclonal antibodies (Zymed Laboratories, San Francisco, CA) and a pan-cadherin mouse monoclonal antibody (Sigma, St. Louis, MO) for 1 h in a moist chamber at room temperature. They were then washed three times in PBS followed by incubation for 45 min with CY-2- or CY-3-conjugated goat anti-rabbit immunoglobulin G or goat anti-mouse immunoglobulin G (Jackson Immunoresearch, West Grove, PA). Cells were washed three times with PBS and mounted in gel mount (Biomeda, Foster City, CA) and examined with a Nikon (Melville, NY) E800 fluorescence microscope.

Metabolic Labeling and Immunoprecipitation

Cultured monolayers of CE cells were plated at 50% confluence on 10-cm dishes. Twelve hours later, cells were washed with methionine-free medium containing dialyzed FBS and then incubated with methionine-free medium containing 150 μCi of [^{35}S]methionine per dish for 18 h at 37°C. After this incubation, the medium was collected, and cells were washed two times with ice-cold PBS (with Ca^{2+} and Mg^{2+}). One milliliter of ice-cold lysis buffer (1% Triton X-100, 0.4% sodium deoxycholate, 0.2% SDS, 150 mM NaCl,

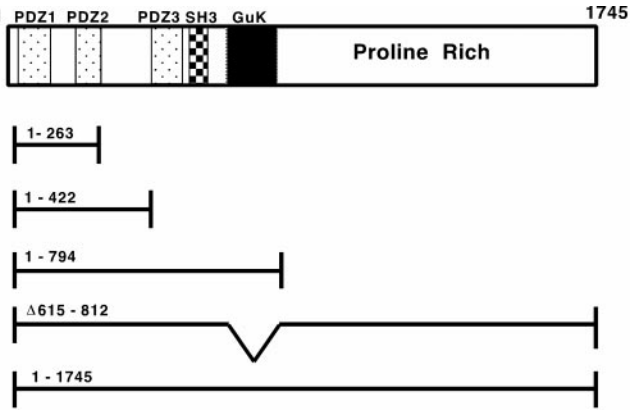

Figure 1. Diagram of mutant ZO-1 proteins. The domain structure of ZO-1 is shown at the top, with the dotted box denoting the boundaries of the PDZ domains, the hatched box the Src homology 3 domain, and the checkered box the GuK domain. Mutants are designated by their amino acids included or deleted (Δ). ZO-$1^{1–263}$, ZO-$1^{1–422}$, ZO-$1^{1–794}$, and ZO-$1^{1–1745}$ (full length) were each tagged with seven c-*myc* epitopes as described in MATERIALS AND METHODS. ZO-$1^{\Delta 615–812}$ (lacking the GuK domain) was tagged with the FLAG epitope.

10 mM HEPES, pH. 7.4, 1 mM phenylmethylsulfonylfluoride, 1 μg/ml pepstatin A, 1 μg/ml leupeptin, 4 μg/ml aprotinin, 1 mM dithiothreitol, and 20 mM benzamidine) was added to each dish, and dishes were rocked back and forth for 30 min at 4°C. Subsequently, cells were scraped into a microcentrifuge tube and centrifuged at 12,000 × *g* for 30 min at 4°C. The supernatants were then mixed with 50 μl of 50% slurry of protein A-Sepharose incubated for 1 h at 4°C and centrifuged for 2 min at 1200 × *g*. Supernatants were transferred to a new tube, and 2 μg of either anti-ZO-1 polyclonal antibody or normal rabbit serum were added and incubated overnight rotating at 4°C. After this incubation, 20 μl of 50% slurry of protein A-Sepharose beads were added to each sample and incubated for 3 h at 4°C. The beads were washed three times in lysis buffer and resuspended in 40 μl 2× sample buffer. The samples were resolved by SDS-PAGE, and the gel was fixed and dried and examined by autoradiography.

Western Blot

Cultured monolayers of CE cells on 10-cm dishes were trypsinized and counted using a hemocytometer. Equal cell numbers were lysed in lysis buffer (see above) and centrifuged at 6000 × *g* for 15 min at 4°C to separate insoluble components. The supernatants were harvested, mixed with 5× sample buffer, and resolved by SDS-PAGE. The separated proteins were electrophoretically transferred to nitrocellulose and incubated in blocking solution (5% dry milk in TBS with 0.2% Tween 20) for 60 min followed by sequential incubations of primary and secondary antibody for 60 min each at room temperature. Proteins were detected by the alkaline phosphatase substrates nitro blue tetrazolium and 5-bromo-4-chloro-3-indolyl phosphate.

RESULTS

Behavior of Truncation Mutants of ZO-1 in Corneal Epithelial Cells

We constructed truncation mutants of ZO-1 with myc or FLAG epitope tags at their C termini as shown in Figure 1. These mutants were stably transfected into rabbit and human corneal cell lines, and their subcellular localization as well as that of endogenous ZO-1 were determined by indirect immunofluorescence. As seen in Figure 2, full-length, epitope-tagged ZO-$1^{1–1745}$ targeted to cell borders (Figure 2A) and colocalized with endogenous ZO-1 (Figure 2B), confirming that the C-terminal epitope tag neither conferred unexpected localization properties on full length ZO-1 nor interfered with endogenous ZO-1 localization. ZO-$1^{1–794}$ also targeted to cell borders (Figure 2C) and colocalized with endogenous ZO-1 (Figure 2D), whereas the localization of ZO-$1^{1–422}$ was diffusely cytoplasmic (Figure 2E). ZO-$1^{1–263}$, with a molecular mass of ~28 kDa, was concentrated in the nucleus (Figure 2G). ZO-$1^{\Delta 615–812}$, which lacks the GuK domain previously implicated in occludin binding (Fanning *et al.*, 1998), localized in a punctate manner, possibly in lysosomes (Figure 2I). The localization and expression of endogenous ZO-1 was not disrupted in any of these stable transfectants (Figure 2, B, D, F, H, and J). These results were consistent in 6–12 independent stable clones isolated for each mutant.

To demonstrate the mobilities and levels of expression of the mutant polypeptides, Western blots were performed on the stably transfected clones. Figure 3 shows the expression of the various mutant proteins, which had electrophoretic mobilities close to their predicted molecular masses as detected by antibodies against their epitope tags. Although all transfected lines displayed steady-state levels of protein, ZO-$1^{1–422}$ and ZO-$1^{1–263}$ cells consistently exhibited higher levels than the others.

N-terminal Regions of ZO-1 Caused a Change in Cell Morphology

Initially it appeared as though none of the mutants disrupted the localization of endogenous ZO-1. However, after ~4–6 wk in culture, stable clones expressing ZO-$1^{1–422}$ and ZO-$1^{1–794}$ underwent a dramatic change in cell morphology, as seen in Figure 4. Although cells expressing ZO-$1^{1–1745}$ (Figure 4, left), ZO-$1^{1–263}$, and ZO-$1^{\Delta 615–812}$ continued to display a cobblestone epithelial morphology, the cells expressing ZO-$1^{1–422}$ and ZO-$1^{1–794}$ became elongated and fibroblast-like in appearance (Figure 4, middle and right). The change in morphology was specific to the clones expressing ZO-$1^{1–422}$ and ZO-$1^{1–794}$, because the phenotype of the other transfectants did not change even after months in culture. The timing necessary for this morphological change was reproducible, because sibling cells retrieved from stocks frozen soon after transfection also required 4–6 wk for this phenotypic change to occur. Transfected cells were thawed on multiple occasions, and single-cell clones were isolated and examined for 4–6 wk to verify the reproducibility of the morphologic change observed. To ensure that this change did not result from the selection of a minor variant, cells were cultured for 1 wk after selection in geneticin. Clones were then isolated by limiting dilution into 96-well plates. The resulting colonies showed a more rapid phenotypic change in 3–5 wk, revealing that the time frame was not sensitive to subcloning.

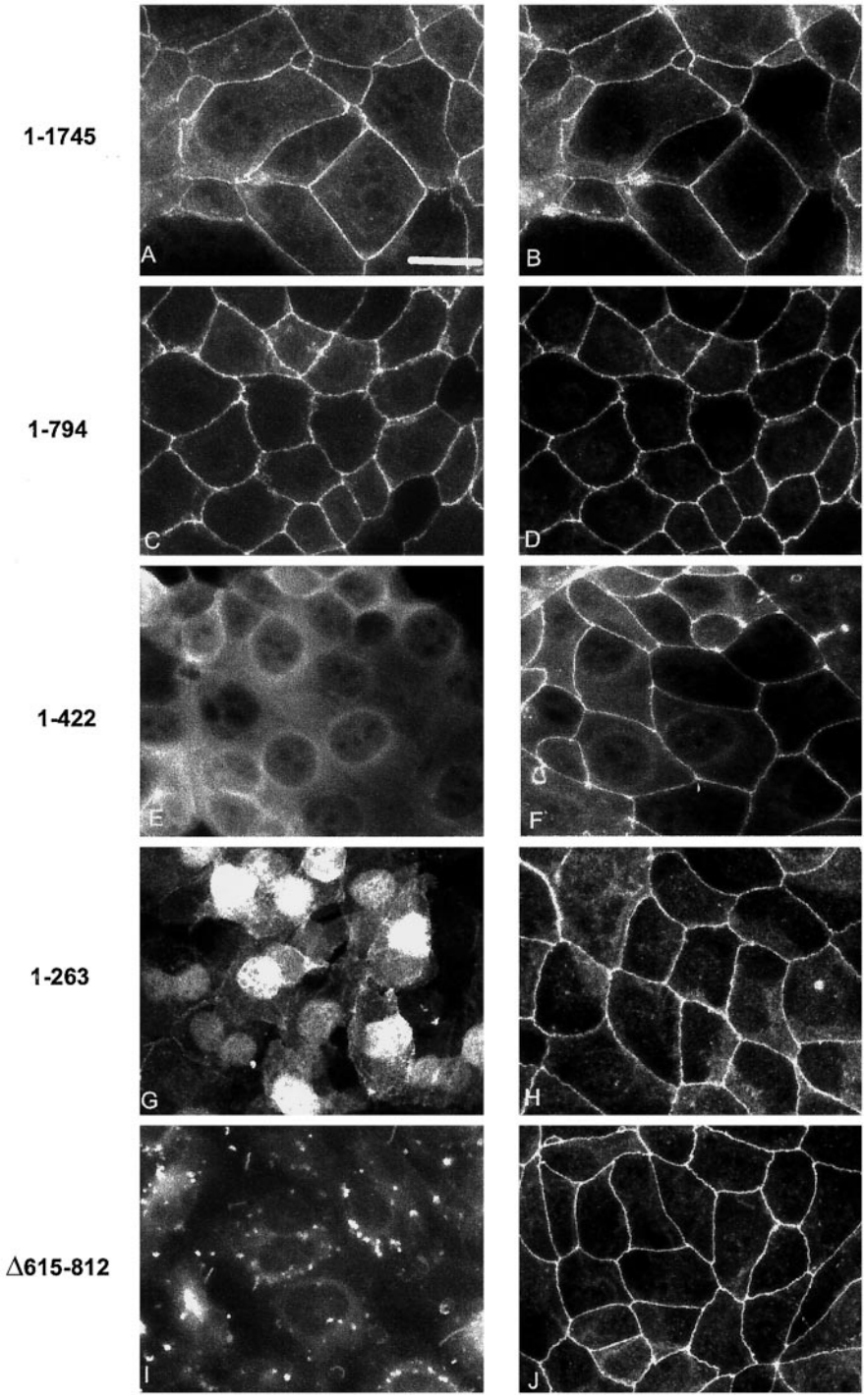

Figure 2. Subcellular distribution of epitope-tagged ZO-1 mutants in corneal epithelial cells. Monolayers of corneal epithelial cells stably expressing truncated ZO-1 proteins were fixed and immunostained. Antibodies against ZO-1 (B, D, F, H, and J) were used to detect the localization of endogenous ZO-1, whereas antibodies to the myc (A, C, E, and G) and FLAG (I) epitope tags demonstrate the subcellular localization of the stably transfected mutant proteins. Bar, 21 μm.

Expression and Localization of Tight Junction Proteins Were Disrupted

The expression of other tight junction proteins was investigated to determine whether ZO-1^{1-422} or ZO-1^{1-794} altered endogenous ZO-1, ZO-2, or occludin levels. Equal cell numbers from cultures that had undergone a morphological change and mock-transfected cells that had not were analyzed by Western blot using antibodies against ZO-1, ZO-2, and occludin. Although there was some decrease in the levels of endogenous ZO-1 and ZO-2, the expression levels of occludin in the morphologically changed cells were dramatically down-regulated (Figure 5).

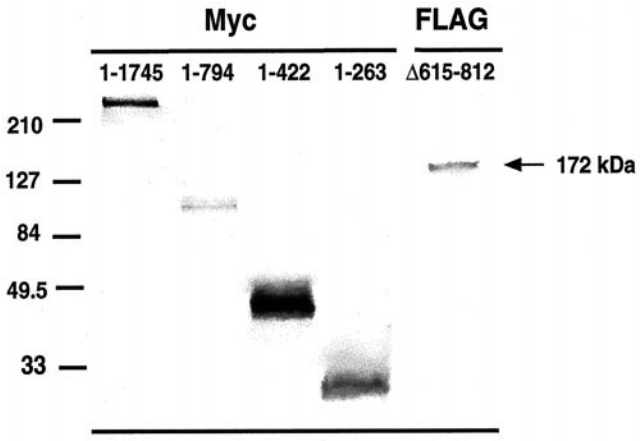

Figure 3. Western blot analysis of whole-cell lysates of stably transfected corneal epithelial cells. Lysates from equal cell numbers of each clone were immunoblotted with myc polyclonal antibody and FLAG monoclonal antibody. Bands of the expected molecular mass for each mutant were detected. Molecular size standards are included on the left (in kilodaltons).

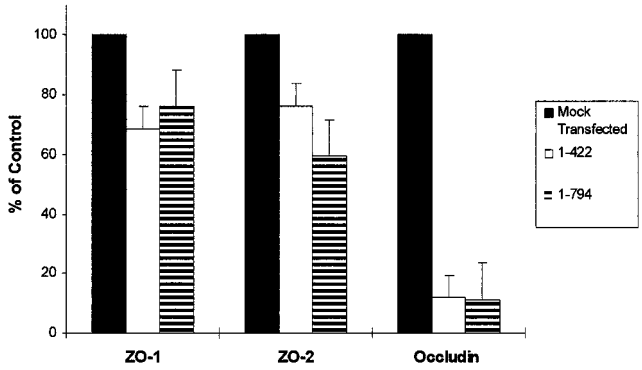

Figure 5. Expression levels of tight junction-associated proteins in the ZO-1^{1-422} and ZO-1^{1-794} cells. The levels of ZO-1, ZO-2, and occludin in these cells were quantitated by densitometric scans of Western blots probed with the indicated antibody. The levels of ZO-1, ZO-2, and occludin in ZO-1^{1-422} cells (white bar) and ZO-1^{1-794} cells (hatched bar) were expressed relative to mock-transfected cells (black bar). The bars represent the mean ± SEM of triplicate determinations.

To examine the subcellular localization of tight and adherens junction proteins, immunofluorescence was performed using ZO-1, ZO-2, occludin, and pan-cadherin antibodies. As demonstrated in Figure 6, these proteins were appropriately localized at cell borders in the parental cells (Figure 6, top row). However, in ZO-1^{1-422} clones, endogenous ZO-1 and ZO-2 were localized cytoplasmically, whereas occludin expression was not detectable above background. The localization of cadherins appeared more disorganized, with many cells showing cytoplasmic staining (Figure 6, middle row). In ZO-1^{1-794} clones, endogenous ZO-1 and cadherins were expressed in a punctate manner at cell borders, suggesting a redistribution of endogenous ZO-1 to adherens junctions. ZO-2 was no longer located at the cell surface and was found in both the cytoplasm and nucleus. As with the ZO-1^{1-422} clones, occludin expression in ZO-1^{1-794} clones was also not detectable above background (Figure 6, bottom row).

Transformation to a Mesenchymal Phenotype

To determine whether the ZO-1^{1-422} and ZO-1^{1-794} clones had undergone an epithelial to mesenchymal transformation

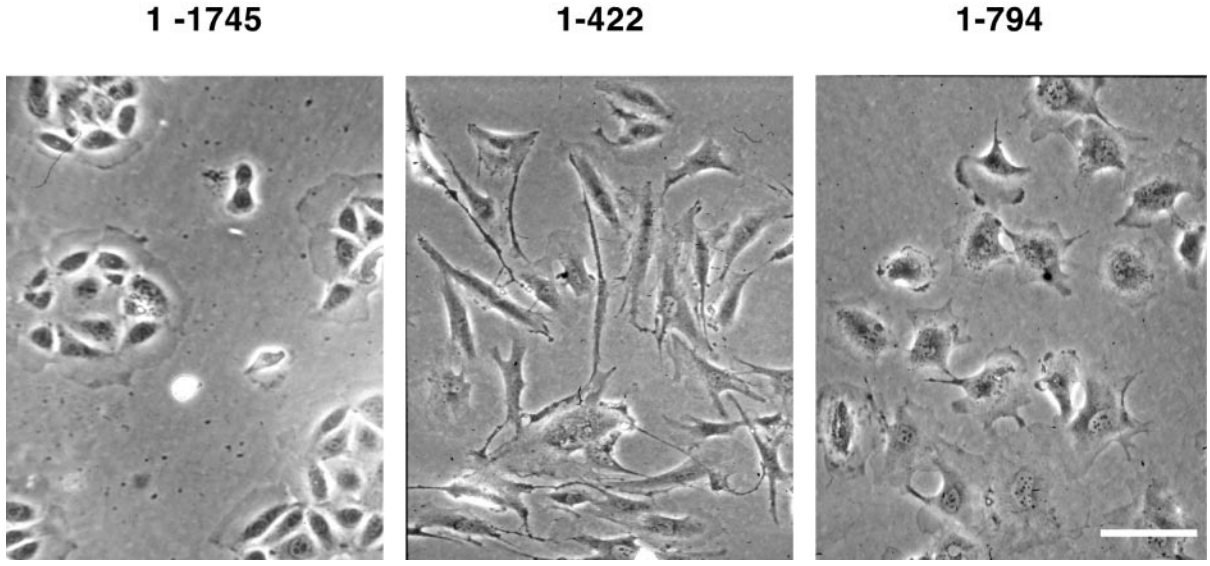

Figure 4. Phase-contrast photomicrographs of stably transfected corneal epithelial cells after 6 wk in culture. Cells containing ZO-1^{1-1745} retain their epithelial morphology. Cells expressing ZO-1^{1-422} display an elongated, spindle-shaped morphology, and ZO-1^{1-794} cells demonstrate a rounded and slightly elongated phenotype. Bar 70 μm.

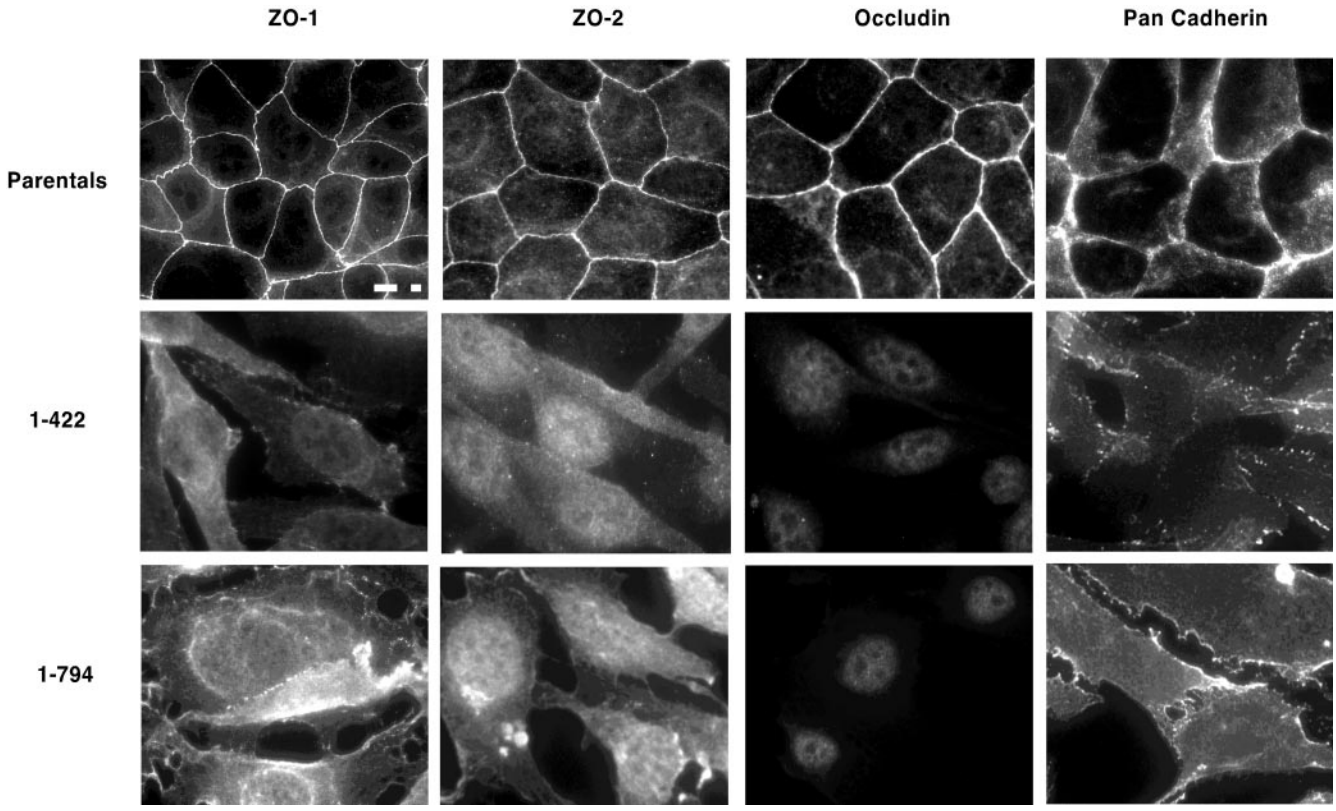

Figure 6. Subcellular localization of tight junction-associated proteins in parental corneal epithelial cells and ZO-1^{1-422} and ZO-1^{1-794} cells. Cell monolayers were fixed and processed for immunofluorescence using antibodies directed against ZO-1, ZO-2, occludin, and pan-cadherins. Parental cells are shown in the top row, ZO-1^{1-422} cells are in the middle row, and ZO-1^{1-794} cells are seen in the bottom row. Bar, 20 μm.

(EMT), the cells were immunostained with antibodies to cytokeratin, vimentin, and smooth muscle actin. As shown in Figure 7, first column, parental corneal epithelial cells expressed a uniform level of the epithelial cell marker cytokeratin (Moll *et al.*, 1982), whereas the levels in clones ZO-1^{1-422} and ZO-1^{1-794} were variable from cell to cell. Expression of vimentin, the intermediate filament protein characteristic of mesenchymal cells (Denk *et al.*, 1983), was absent in the parental cells but was abundantly expressed in clones ZO-1^{1-422} and ZO-1^{1-794} (Figure 7, middle column). Similarly, smooth muscle actin, although absent from parental cells, was highly expressed in clones ZO-1^{1-422} and ZO-1^{1-794} (Figure 7, third column). These data imply that ZO-1^{1-422} and ZO-1^{1-794} have undergone at least a partial transformation from an epithelial to a mesenchymal cell (Savagner *et al.*, 1997).

Immunoprecipitation of Endogenous ZO-1 in Transformed and Parental Cells

A possible interaction of endogenous ZO-1 with novel proteins in the ZO-1^{1-422} and ZO-1^{1-794} cells was examined by metabolic labeling and immunoprecipitation in nondenaturing conditions. As shown in Figure 8, mock-transfected corneal epithelial cells displayed a pair of bands labeled with equal intensities. This doublet was confirmed to be ZO-1 by Western blot analysis of the immunoprecipitated samples probed with a ZO-1 antibody (our unpublished data). Although ZO-1^{1-422} and ZO-1^{1-794} cells also displayed doublets in their ZO-1 immunoprecipitates (Figure 8), there was a difference in the relative intensity of the two bands with a stronger lower band. There was also a unique band of ~55 kDa (Figure 8, asterisk) that appeared in the immunoprecipitated samples of ZO-1^{1-422} cells.

DISCUSSION

In the current study, we have identified two truncation mutants of ZO-1 (ZO-1^{1-422} and ZO-1^{1-794}) that mediated a dramatic change in cell morphology 4–6 wk after transfection into corneal epithelial cells. These two N-terminal mutants of ZO-1 uniquely overlapped in the region between PDZ2 and -3, which was absent in the other truncation mutants that had no effect on cell morphology. After a 4- to 6-wk latent period, the cells transfected with ZO-1^{1-422} and ZO-1^{1-794} displayed a fibroblast-like, elongated appearance unlike either parental cells or clones transfected with ZO-1^{1-1745}, ZO-$1^{\Delta 615-812}$, or ZO-1^{1-263}, which continued to show an epithelial cobblestone morphology. Upon observation of a phenotypic change in cells expressing ZO-1^{1-422}, constructs ZO-1^{1-263} and ZO-$1^{263-422}$ were generated to deter-

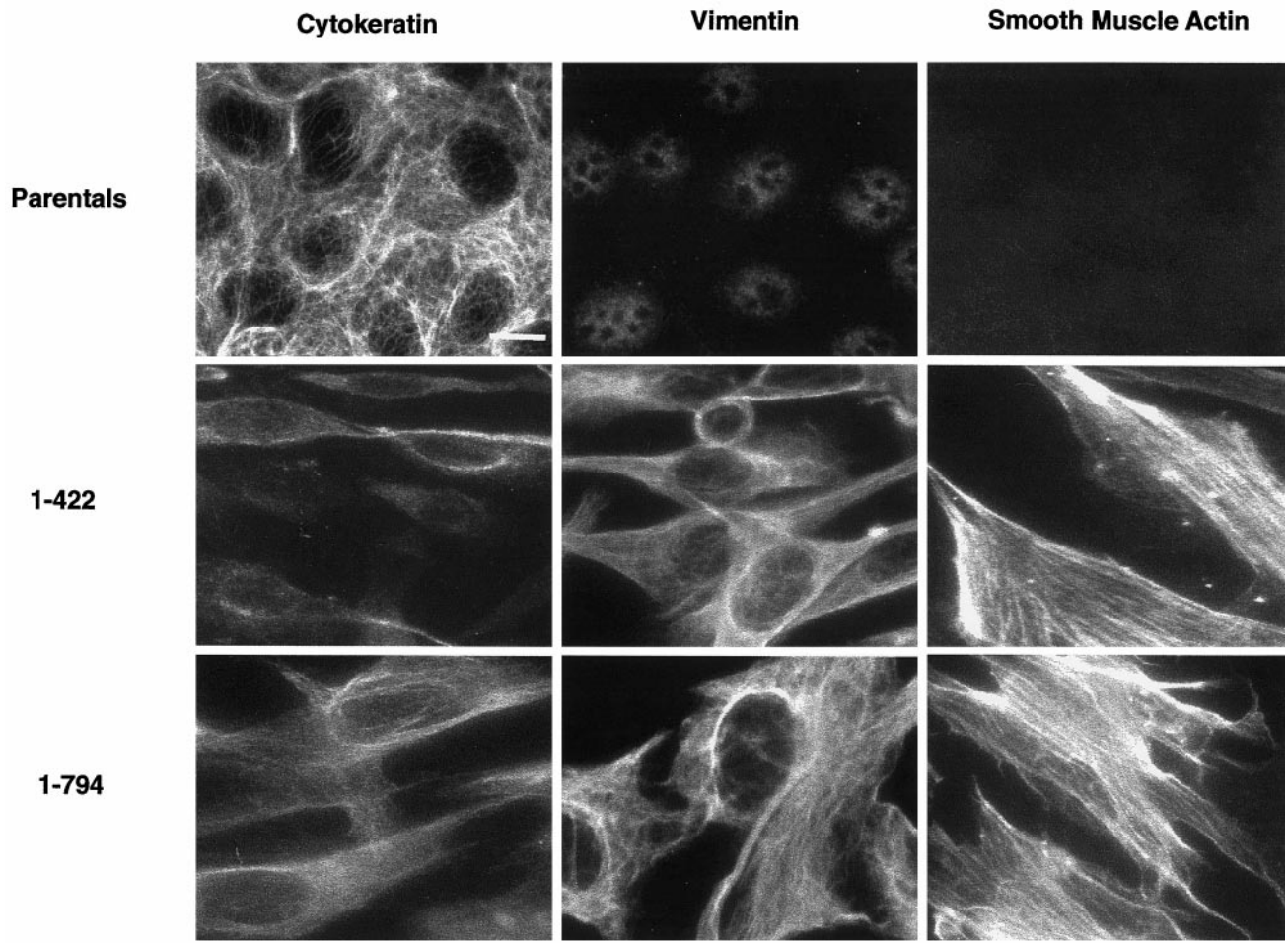

Figure 7. ZO-1^{1-422} and ZO-1^{1-794} cells express mesenchymal markers. Parental cells (top row), ZO-1^{1-422} cells (middle row), and ZO-1^{1-794} cells (bottom row) cells were fixed and immunostained with antibodies to cytokeratin, an epithelial cell marker (left column) and both vimentin (middle column) and smooth muscle actin (right column) mesenchymal cell markers. Bar, 20 μm.

mine the smallest domain of ZO-1 that could induce this morphological change. As previously described, ZO-1^{1-263} maintained an epithelial morphology, whereas attempts to stably express ZO-$1^{263-422}$ were unsuccessful, because cells transfected with this construct died during selection. This suggests the possibility that this region of ZO-1, between the PDZ2 and -3 domains, may be responsible for inducing this mesenchymal-like transformation.

To characterize the phenotypic change from an epithelial to a fibroblast-like morphology caused by ZO-1^{1-422} and ZO-1^{1-794}, these cells were examined for their expression of various epithelial and mesenchymal markers. The transformation observed was a partial transformation, as evidenced by the up-regulation of mesenchymal markers such as vimentin and smooth muscle actin and the inconsistent, variable expression of cytokeratins (Savagner *et al.*, 1997). Cells expressing ZO-1^{1-422} and ZO-1^{1-794} lacked tight junctions and had no measurable transepithelial resistance compared with mock transfected parental cells and ZO-1^{1-1745} (128.1 $\pm$ 3.8 Ω/cm^2).

Tight junction-associated proteins such as ZO-1, ZO-2, and occludin no longer localized at cell borders but were found throughout the cytoplasm and were down-regulated in their expression. To examine whether endogenous ZO-1 in these transformed cells was altered, the transformed cells were metabolically labeled and immunoprecipitated with ZO-1 antibodies. As seen in Figure 8, immunoprecipitation of endogenous ZO-1 in cells expressing ZO-1^{1-422} demonstrates coprecipitation of a novel band of ~55 kDa. This suggests the possibility that endogenous ZO-1 interacted with a novel protein as a result of this transformation, which may have played a role in the induction of this mesenchymal-like phenotype. It is also of interest that the immunoprecipitated ZO-1 doublet had differing intensities compared with that of the mock-transfected cells. The lower band was more intense in the transformed cells, suggesting the possibility of less-phosphorylated ZO-1 in these cells. This is consistent with studies demonstrating that Madin–Darby canine kidney cells maintained in low calcium with no tight junctions have an altered distribution of ZO-1 as

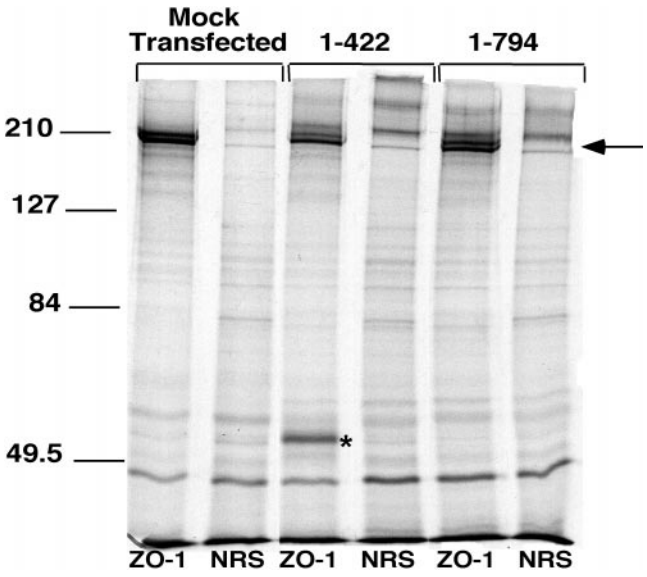

Figure 8. ZO-1 immunoprecipitation of [^{35}S]methionine-labeled cells. Equivalent cell lysates from mock-transfected cells and ZO-1^{1-422} and ZO-1^{1-794} cells were immunoprecipitated with a ZO-1 polyclonal antibody (ZO-1) or control normal rabbit serum (NRS). An arrow denotes a ZO-1 doublet in all three cell lines, and an asterisk denotes a novel band of ~55 kDa that coprecipitates with ZO-1 in ZO-1^{1-422} cells. Molecular size standards are included on the left (in kilodaltons).

well as lower total phosphorylation of ZO-1 (Howarth *et al.*, 1994).

Although ZO-1^{1-422} and ZO-1^{1-794} both caused a partial mesenchymal transformation, the morphologies of these transfected cells were different from each other. Cells transformed with ZO-1^{1-422} were more elongated and spindle-like and lacked adherens junctions, as judged by immunostaining with a pan-cadherin antibody. However ZO-1^{1-794}-expressing cells, although fibroblast-like, were more rounded and demonstrated punctate cadherin expression, as has been shown in cultured fibroblasts (Itoh *et al.*, 1991). Endogenous ZO-1 appeared to be colocalized with cadherins in the cells transfected with ZO-1^{1-794}.

The most puzzling aspect of this dramatic phenotypic change was the length of time necessary for the phenomenon to occur. After isolating single clones from stable transfections, the cells were cultured for ~4–6 wk with passage twice weekly before they underwent their morphological change. This time frame was not sensitive to subcloning, in that transfectants that were allowed to expand in culture before subcloning required a proportionately shorter time to affect the phenotypic change.

The 4- to 6-wk time frame complicates an exploration into the mechanisms of action of the mutants. Transforming growth factor β3 (TGFβ3) has been demonstrated to promote a transformation from epithelium to mesenchyme of progenitor cells of the heart valves, which arise from the endothelial cells in the atrioventricular canal (Potts *et al.*, 1991; Runyan *et al.*, 1992). Similarly, TGFβ3 also promotes EMT of rodent (Kaartinen *et al.*, 1997) and chicken palate medial edge epithelia within 24–72 h after addition to cultured palates (Sun *et al.*, 1998). To investigate whether the transformed clones had become more susceptible to TGFβ3, the time course of TGFβ3-induced EMT was studied in the corneal cells by placing the parental cells in 100 ng/ml TGFβ3. We observed that the parental cells underwent EMT within 5 d of TGFβ3 application, indicating that this growth factor operated at a much more rapid time scale than that shown by the ZO-1 mutants (our unpublished data). However, when 0.1–10 ng/ml TGF β3 was added to cells immediately after transfection with ZO-1^{1-422} and ZO-1^{1-794}, the cells did not undergo the morphological change within the 7 d they were treated (our unpublished data). These data imply that stable expression of ZO-1^{1-422} and ZO-1^{1-794} did not cause the cells to become more susceptible to the growth factor. Conditioned medium, harvested from ZO-1^{1-422} and ZO-1^{1-794} cells in culture for >1 mo, and okadaic acid, a potent phosphatase 2A inhibitor, did not cause EMT in the parental cells (our unpublished data), indicating that these agents were not active in inducing EMT in this cell type.

Another possible model to explain the delay in partial mesenchymal transformation was the necessity for the levels of endogenous ZO-1 to be greatly reduced before ZO-1^{1-422} and ZO-1^{1-794} were able to exert their effect. However, comparison of parental cells with stably transfected cells before and after the epithelial–mesenchymal transformation revealed no significant differences in endogenous ZO-1 levels (our unpublished data).

ZO-1^{1-422} and ZO-1^{1-794} cells were cocultured with parental corneal epithelial cells at a 4:1 ratio. The ZO-1^{1-422} and ZO-1^{1-794} cells grew on top of the parental cells and clumped together, whereas the parental cells proliferated rapidly and formed a confluent monolayer under the clumped cells after 4 d in culture. There was no reversion of the ZO-1^{1-422} and ZO-1^{1-794} cells back to an epithelial-like morphology, nor did they cause the parental cells to undergo a similar mesenchymal transformation (our unpublished data).

Epithelial cells transfected with constitutively active Ras become elongated and fibroblast-like but revert back to an epithelial cell morphology when the Ras pathway is inhibited (Y.-H. Chen, personal communication). An inhibitor of the Ras signaling pathway, PD 098059 (Alessi *et al.*, 1995), was added to ZO-1^{1-422} and ZO-1^{1-794} cells to investigate whether the Ras pathway was involved in this morphological change and whether these cells would revert back to an epithelial cell phenotype. However, PD 098059, which acts within 24 h on Ras-transformed Madin–Darby canine kidney epithelial cells (Y.H. Chen, personal communication), had no detectable effect on ZO-1^{1-422} and ZO-1^{1-794} cells after 3 d in culture (our unpublished data). Similarly, okadaic acid and TGFβ3 did not cause a phenotypic reversion.

Although the length of time necessary between expression of ZO-1^{1-422} and that of ZO-1^{1-794} in corneal epithelial cells and the appearance of a transformed phenotype suggested a complex signaling pathway, the effect was specific to these two ZO-1 N-terminal mutants. The morphological change was not due to expression levels of the mutant proteins, because independent clones of ZO-1^{1-422} and ZO-1^{1-794} varied in their levels of expression up to threefold. ZO-1^{1-422} and ZO-1^{1-794} lacked the proline-rich C terminus of ZO-1 that has been shown to bind actin filaments (Itoh *et al.*, 1997; Fanning *et al.*, 1998). Without this cytoskeletal anchor, the

mutants may have been free to interact with proteins normally not accessible to full-length ZO-1. Further studies will be necessary to elucidate the binding partners and the signaling pathways activated by these ZO-1 truncation mutants.

REFERENCES

Alessi, D.R., Cuenda, A., Cohen, P., Dudley, D.T., and Saltiel, A.R. (1995). PD 098059 is a specific inhibitor of the activation of mitogen-activated protein kinase kinase in vitro and in vivo. J. Biol. Chem. *270*, 27489–27494.

Anderson, J.M. (1996). Cell signaling: MAGUK magic. Curr. Biol. *6*, 382–384.

Anderson, J.M., Balda, M.S., and Fanning, A.S. (1993). The structure and regulation of tight junctions. Curr. Opin. Cell Biol. *5*, 772–778.

Anderson, J.M., and Van Itallie, C.M. (1995). Tight junctions and the molecular basis for regulation of paracellular permeability. Am. J. Physiol. *269*, G467–G475.

Araki, K., Ohashi, Y., Sasabe, T., Kinoshita, S., Hayashi, K., Yang, X.Z., Hosaka, Y., Aizawa, S., and Handa, H. (1993). Immortalization of rabbit corneal epithelial cells by a recombinant SV40-adenovirus vector. Invest. Ophthalmol. Vis. Sci. *34*, 2665–2671.

Araki-Sasaki, K., Ohashi, Y., Sasabe, T., Hayashi, K., Watanabe, H., Tano, Y., and Handa, H. (1995). An SV40-immortalized human corneal epithelial cell line and its characterization. Invest. Ophthalmol. Vis. Sci. *36*, 614–621.

Balda, M.S., Whitney, J.A., Flores, C., Gonzalez, S., Cereijido, M., and Matter, K. (1996). Functional dissociation of paracellular permeability and transepithelial electrical resistance and disruption of the apical-basolateral intramembrane diffusion barrier by expression of a mutant tight junction membrane protein. J. Cell Biol. *134*, 1031–1049.

Beatch, M., Jesaitis, L.A., Gallin, W.J., Goodenough, D.A., and Stevenson, B.R. (1996). The tight junction protein ZO-2 consists of three PDZ domains and an alternatively spliced region. J. Biol. Chem. *271*, 25723–25726.

Chen, Y.H., Merzdorf, C., Paul, D.L., and Goodenough, D.A. (1997). COOH terminus of occludin is required for tight junction barrier function in early *Xenopus* embryos. J. Cell Biol. *138*, 891–899.

Cho, K.O., Hunt, C.A., and Kennedy, M.B. (1992). The rat brain postsynaptic density fraction contains a homolog of the *Drosophila discs-large* tumor suppressor protein. Neuron *9*, 929–942.

Citi, S. (1993). The molecular organization of tight junctions. J. Cell Biol. *121*, 485–489.

Denk, H., Krepler, R., Artlieb, U., Gabbiani, G., Rungger-Brandle, E., Leoncini, P., and Franke, W.W. (1983). Proteins of intermediate filaments. An immunohistochemical and biochemical approach to the classification of soft tissue tumors. Am. J. Pathol. *110*, 193–208.

Denker, B.M., and Nigam, S.K. (1998). Molecular structure and assembly of the tight junction. Am. J. Physiol. *274*, F1–F9.

Fanning, A.S., Jameson, B.J., Jesaitis, L.A., and Anderson, J.M. (1998). The tight junction protein ZO-1 establishes a link between the transmembrane protein occludin and the actin cytoskeleton. J. Biol. Chem. *273*, 29745–29753.

Fujimoto, K. (1995). Freeze-fracture replica electron microscopy combined with SDS digestion for cytochemical labeling of integral membrane proteins. Application to the immunogold labeling of intercellular junctional complexes. J. Cell Sci. *108*, 3443–3449.

Furuse, M., Fujimoto, K., Sato, N., Hirase, T., Tsukita, S., and Tsukita, S. (1996). Overexpression of occludin, a tight junction-associated integral membrane protein, induces the formation of intracellular multilamellar bodies bearing tight junction-like structures. J. Cell Sci. *109*, 429–435.

Furuse, M., Fujita, K., Hiiragi, T., Fujimoto, K., and Tsukita, Sh. (1998a). Claudin-1 and -2: novel integral membrane proteins localizing at tight junctions with no sequence similarity to occludin. J. Cell Biol. *141*, 1539–1550.

Furuse, M., Hirase, T., Itoh, M., Nagafuchi, A., Yonemura, S., Tsukita, S., and Tsukita, S. (1993). Occludin: a novel integral membrane protein localizing at tight junctions. J. Cell Biol. *123*, 1777–1788.

Furuse, M., Sasaki, H., Fujimoto, K., and Tsukita, S. (1998b). A single gene product, claudin-1 or -2 reconstitutes tight junction strands and recruits occludin in fibroblasts. J. Cell Biol. *143*, 391–401.

Goodenough, D.A. (1999). Plugging the leaks. Proc. Natl. Acad. Sci. USA *96*, 319–321.

Haskins, J., Gu, L., Wittchen, E.S., Hibbard, J., and Stevenson, B.R. (1998). ZO-3, a novel member of the MAGUK protein family found at the tight junction, interacts with ZO-1 and occludin. J. Cell Biol. *141*, 199–208.

Howarth, A.G., Hughes, M.R., and Stevenson, B.R. (1992). Detection of the tight junction-associated protein ZO-1 in astrocytes and other nonepithelial cell types. Am. J. Physiol. *262*, C461–C469.

Howarth, A.G., Singer, K.L., and Stevenson, B.R. (1994). Analysis of the distribution and phosphorylation state of ZO-1 in MDCK and nonepithelial cells. J. Membr. Biol. *137*, 261–270.

Itoh, M., Nagafuchi, A., Moroi, S., and Tsukita, S. (1997). Involvement of ZO-1 cadherin-based cell adhesion through its direct binding to α catenin and actin filaments. J. Cell Biol. *138*, 181–192.

Itoh, M., Yonemura, S., Nagafuchi, A., Tsukita, S., and Tsukita, S. (1991). A 220-kD undercoat-constitutive protein: Its specific localization at cadherin-based cell-cell adhesion sites. J. Cell Biol. *115*, 1449–1462.

Kaartinen, V., Cui, X., Heisterkamp, N., Groffen, J., and Shuler, C.F. (1997). Transforming growth factor-β3 regulates transdifferentiation of medial edge epithelium during palatal fusion and associated degradation of the basement membrane. Dev. Dyn. *209*, 255–260.

Kim, E., Niethammer, M., Rothschild, A., Jan, Y.N., and Sheng, M. (1995). Clustering of Shaker-type K^+ channels by interaction with a family of membrane-associated guanylate kinases. Nature *378*, 85–88.

Kim, S. (1995). Tight junctions, membrane-associated guanylate kinases and cell signaling. Curr. Biol. *7*, 641–649.

McCarthy, K.M., Skare, I.B., Stankewich, M.C., Furuse, M., Tsukita, S., Rogers, R.A., Lynch, R.D., and Schneeberger, E.E. (1996). Occludin is a functional component of the tight junction. J. Cell Sci. *109*, 2287–2298.

Moll, R., Franke, W.W., Schiller, D.L., Geiger, B., and Krepler, R. (1982). The catalog of human cytokeratins: patterns of expression in normal epithelia, tumors and cultured cells. Cell *31*, 11–24.

Morita, K., Furuse, M., Fujimoto, K., and Tsukita, S. (1999). Claudin multigene family encoding four-transmembrane domain protein components of tight junction strands. Proc. Natl. Acad. Sci. USA *96*, 511–516.

Potts, J.D., Dagle, J.M., Walder, J.A., Weeks, D.L., and Runyan, R.B. (1991). Epithelial-mesenchymal transformation of embryonic cardiac endothelial cells is inhibited by a modified antisense oligodeoxynucleotide to transforming growth factor beta 3. Proc. Natl. Acad. Sci. USA *88*, 1516–1520.

Ren, R., Mayer, B.J., Cicchetti, P., and Baltimore, D. (1993). Identification of a ten-amino acid proline-rich SH3 binding site. Science *259*, 1157–1161.

Runyan, R.B., Potts, J.D., and Weeks, D.L. (1992). TGF-beta 3-mediated tissue interaction during embryonic heart development. Mol. Reprod. Dev. *32*, 152–159.

Savagner, P., Yamada, K.M., and Thiery, J.P. (1997). The zinc-finger protein slug causes desmosome dissociation, an initial and necessary step for growth factor-induced epithelial-mesenchymal transition. J. Cell Biol. *137*, 1403–1419.

Simon, D.B., *et al*. (1999). Paracellin-1, a renal tight junction protein required for paracellular Mg^{2+} resorption. Science *285*, 103–106.

Songyang, Z., Fanning, A.S., Fu, C., Xu, J., Marfatia, S.M., Chishti, A.H., Crompton, A., Chan, A.C., Anderson, J.M., and Cantley, L.C. (1997). Recognition of unique carboxyl-terminal motifs by distinct PDZ domains. Science *275*, 73–76.

Stevenson, B., Siliciano, J.D., Mooseker, M.S., and Goodenough, D.A. (1986). Identification of ZO-1: a high molecular weight polypeptide associated the tight junction (zonula occludens) in a variety of epithelia. J. Cell Biol. *103*, 755–766.

Stevenson, B.R., and Keon, B.K. (1998). The tight junction: morphology to molecules. Annu. Rev. Cell Dev. Biol. *14*, 89–109.

Sun, D., Vanderburg, C.R., Odierna, G.S., and Hay, E.D. (1998). TGFβ3 promotes transformation of chicken palate medial edge epithelium to mesenchyme in vitro. Development *125*, 95–105.

Willott, E., Balda, M.S., Fanning, A.S., Jameson, B., Van Itallie, C., and Anderson, J.M. (1993). The tight junction protein ZO-1 is homologous to the *Drosophila* discs-large tumor suppressor protein of septate junctions. Proc. Natl. Acad. Sci. USA *90*, 7834–7838.

Wong, V., and Gumbiner, B.A. (1997). A synthetic peptide corresponding to the extracellular domain of occludin perturbs the tight junction permeability barrier. J. Cell Biol. *136*, 399–409.